A millennial record of environmental change in peat deposits from the Misten bog (East Belgium)

Francois de Vleeschouwer, Anna Pazdur, Cédric Luthers, Maurice Streel, Dmitri Mauquoy, Cécile Wastiaux, Gaël Le Roux, Robert Moschen, Maarten Blaauw, Jacek Pawlyta, et al.

A millennial record of environmental change in peat deposits from the Misten bog (East Belgium)

François De Vleeschouwer [a,*], Anna Pazdur [a], Cédric Luthers [b], Maurice Streel [b], Dmitri Mauquoy [c], Cécile Wastiaux [d], Gaël Le Roux [e,1], Robert Moschen [f], Maarten Blaauw [g], Jacek Pawlyta [a], Jarek Sikorski [a], Natalia Piotrowska [a]

[a] GADAM Centre, Institute of Physics, Silesian University of Technology, Gliwice, Poland
[b] U.R. Paléobotanique, Paléopalynologie et Micropaléontologie, Géologie, ULg, Liège, Belgium
[c] School of Geosciences, University of Aberdeen, Aberdeen, United Kingdom
[d] Station Scientifique des Hautes Fagnes, ULg, Robertville, Belgium
[e] U.R. Argiles, Géochimie et Environnements Sédimentaires, Géologie, ULg, Liège, Belgium
[f] Institute of Bio- and Geosciences 3: Agrosphere, Jülich Research Centre, Germany
[g] School of Geography, Archaeology and Palaeoecology, Queen's University Belfast, United Kingdom

A B S T R A C T

In this study, palaeoenvironmental changes recorded in the top metre of a peat profile (Misten bog, East Belgium) were investigated using a multiproxy approach. Proxies include bulk density, Ti and Si content, pollen, macrofossils, $\delta^{13}C$ on specific *Sphagnum* stems, and $\delta^{13}C$–$\delta^{18}O$ on *Sphagnum* leaves. A high-resolution chronology was generated using ^{210}Pb measurements and 22 ^{14}C AMS dates on carefully selected *Sphagnum* macrofossils. $\delta^{13}C$ only records large change in mire surface wetness. This is partly due to the fact that the core was taken from the edge of a hummock, which may make it difficult to track small isotopic changes. The $\delta^{13}C$ signal seems to be dependent upon the *Sphagnum* species composition. For example, a change between *Sphagnum* section *Cuspidata* towards *Sphagnum imbricatum* causes a significant drop in the $\delta^{13}C$ values. On the whole, the C and O isotopes record two shallow pool phases during the 8th–9th and the 13th centuries. Pollen and atmospheric soil dust (ASD) fluxes records increased human occupation in the area. There may be some climatic signals in the ASD flux, but they are difficult to decipher from the increasing human impact (land clearance, agriculture) during the last millennium. The variations in the proxies are not always synchronous, suggesting different triggering factors (temperature, wetness, windiness) for each proxy. This study also emphasizes that, compared to studies dealing with pollution using geochemical proxies, palaeoclimatic inferences from peat bogs need as many proxies as possible, together with highly accurate and precise age-models, in order to better understand climate variability and their consequences during the Holocene.

1. Introduction

Tracking environmental changes in peat bogs during the Holocene, and more specifically in the last millennium, is relatively complex, because this period has seen human impacts superimposed upon abrupt climatic changes, often resulting in complex palaeoenvironmental signals. Given this, the need for multiproxy approaches has been emphasized in recent studies (e.g. Yeloff and Mauquoy, 2006; Barber, 2007; Blaauw et al., 2010a). However, although some studies show synchronous changes in either climate- or human-driven changes (see e.g. discussion in Barber, 2007), others show discrepancies in the timing of events (e.g. Charman et al., 2009; De Vleeschouwer et al., 2009).

In peat bogs, short-term (*i.e.* less than 100 years) events are difficult to date with precision because very high-resolution chronologies are required. This focus on dating control is rarely undertaken because dating effort is often concentrated on long-term trends in peat stratigraphy. This is problematic, because less attention is given to high-resolution dating of abrupt, short-term events, which are crucial for a better understanding of their link with climate variations and cycles, and their impact on the environment. Moreover, the potential to generate very high-resolution

doi:10.1016/j.quaint.2011.12.010

chronologies by modern AMS radiocarbon techniques using aboveground plant macrofossils (Mauquoy et al., 2008) offers the possibility to go beyond the Holocene trend and focus on abrupt, short-term events by analysing a greater number of thinner peat slices (Amesbury et al., 2010) and by concentrating an increased number of dates within a limited time period (e.g. Mauquoy et al., 2002; Blaauw et al., 2007). On the other hand, there has been recent discussion on whether it is possible to obtain centennial or decadal resolution using peat archives (e.g. Barber, 2007; Amesbury et al., 2010), mainly because the age-model, as well as the number of dated intervals, will greatly influence the final age resolution. In most cases, because calibrated dates often have asymmetric probability distributions spanning decades to centuries, a mean age derived from an age-model will not always represent the most probable age. Recent advances in age-modelling (e.g. Blaauw et al., 2011, 2004), and critical assessment of event synchroneity (e.g. Blaauw et al., 2007, 2010b; Charman et al., 2009) has pushed forward the need for, if not higher resolution, more accurate ways of representing the chronologies of proxies, in order to best determine 1) the time interval of a single event and 2) the minimal resolution that could be obtained in a peat core.

This paper proposes to assess accurate time intervals to a series of events recorded in proxies, triggered by either human or climatic factors, in a peat core from Belgium. In the Hautes Fagnes (East Belgium), previous studies have already demonstrated the potential of peat archives for reconstructing atmospheric pollution (e.g. De Vleeschouwer et al., 2007) or regional vegetation change (e.g. Persh, 1950; Damblon, 1994). To date, however, there is a clear lack of high-resolution and well-dated multiproxy palaeoenvironmental reconstructions spanning the last millennium in this area. This is crucial in order to improve understanding of past climatic changes for this part of Europe, as the Hautes Fagnes are situated in a key position among European peat deposits, under both oceanic and continental influences. The objectives of this research are: (1) to distinguish natural from anthropogenic signals using a very high-resolution chronology and a trans-disciplinary, multiproxy approach; (2) to identify abrupt climatic changes from the long-term trends; and (3) to identify the nature of climatic changes, *i.e.* wetter or drier, warmer or colder, more or less windy. This is achieved by studying a 1-m *Sphagnum*-dominated peat core using various proxies: pollen, plant macrofossils, stable carbon and oxygen isotopes, titanium (Ti) and silicon (Si) contents, and ^{14}C–^{210}Pb dating. Besides the main objectives, this study also aims to better understand the role of *Sphagnum* species composition on the $\delta^{13}C$ signal and to improve understanding of the $\delta^{18}O$ signal in *Sphagnum* mosses.

2. Site location

The Misten bog is located in the Hautes Fagnes Plateau (East Belgium, Fig. 1). The average precipitation is *c.* 1440 mm/y and the mean annual temperature over the Hautes Fagnes averages 6.7 °C (Mormal and Tricot, 2004). The area contains several peat deposits, parts of which are ombrotrophic. The Misten bog (50°33′50″N, 06°09′50″E, 620 m a.s.l.) contains some of the deepest peat deposits of this area, with more than 7 m of peat in its centre (Fig. 1). It was drained from its northern to its southern border by a single ditch dug in 1774 AD (see Nekrassoff, 2007), and subsequently moderately dammed around 1970. The outer rim of the bog has also been cut, mainly in the northeastern and southeastern edges. The first cuttings took place around the XIVth century and were of very small scale (Hindryckx and Streel, 2000). Intensification of cutting took place during the XVIIth and XVIIIth centuries and stopped during the Second World War. These systematic cuttings may have affected the bog hydrology since the middle of the XVIIIth century. However, the extent of damage towards the centre of the bog, where the core was taken, remains unclear (Hindryckx, 2000; Hindryckx and Streel, 2000).

Several features confirm the ombrotrophic nature of the Misten bog. First, it is located on an isolated plateau (see Fig. 1), which prevents the bog from receiving lateral mineral inputs, e.g. through small streams. The bog vegetation is mainly composed of *Sphagnum* spp., built up into low hummocks, which is also characteristic of ombrotrophic systems. However, the surface *Sphagnum* vegetation

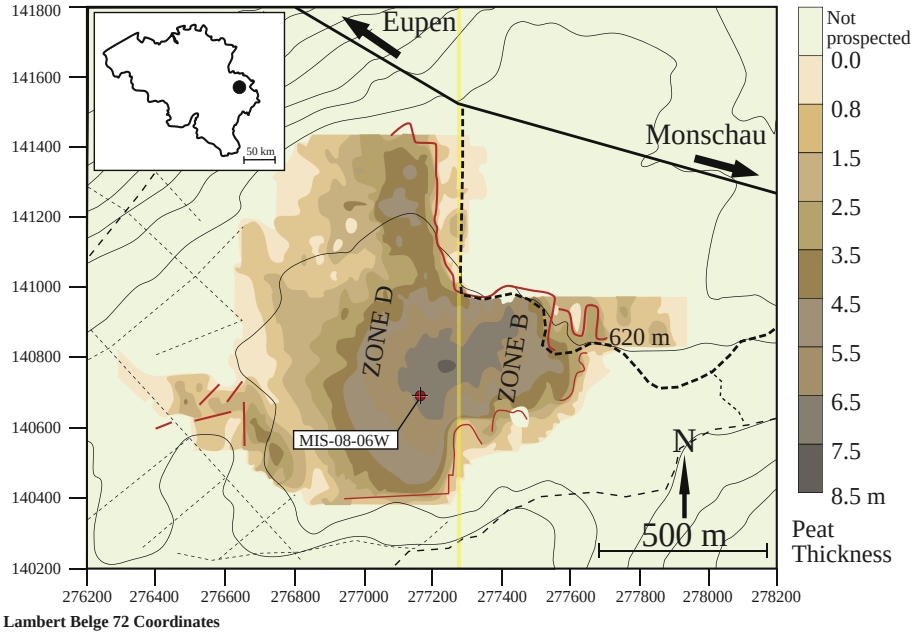

Fig. 1. The Misten bog (south of the Eupen-Monschau road) and the location of the MIS-08-06W peat profile. Peat thickness after Wastiaux and Schumacker (2003). Dotted lines are access pathways. Red lines are the cutting fronts (stopped during the 2nd world war). The yellow stripe represents the main drain, dug in 1774 and active until 1970). (For interpretation of the references to colour in this figure legend, the reader is referred to the web version of this article.)

has been recently invaded by abundant amounts of *Erica tetralix*, *Calluna vulgaris* and *Vaccinium* spp. shrubs, reflecting the recent drying of the bog and its evolution towards a peat moor. Geochemical analyses also confirm ombrotrophy (De Vleeschouwer et al., 2007). Finally, the plant macrofossil record of the entire core (see Fig. 4) is also consistent with the presence of acidic, nutrient-poor conditions characteristic of ombrotrophic peat bogs.

3. Materials and methods

3.1. Coring and subsampling

A 1-m core was retrieved from the centre of Misten bog (Fig. 1) in February 2008 using a plain titanium 15 × 15 × 100 cm Wardenaar corer (Wardenaar, 1986). The peat profile was collected from the edge of a hummock, in order to register a maximum of vegetation change in the profile. The core was then wrapped in plastic film and placed into a wooden box with the same dimensions to allow for safe transport. Peat samples were stored in a freezer (−20 °C) at the Institute of Earth Sciences (University of Heidelberg, Germany) and sub-sampled soon after. The core was sliced frozen using a stainless steel band saw at the Institute of Earth Sciences (University of Heidelberg, Germany) with a *c.* 1 cm increment. The thickness of each slice was then measured again to estimate the loss due to the slicing and to subsequently correct the mid-point depth of each sample. The edges of each slice were removed to avoid any metal contamination by the saw. Each slice was then sub-sampled to provide enough material for each analysed proxy. All the sub-samples were stored in plastic bags in a freezer prior to transfer to the respective laboratories.

3.2. Chronology of the core

The chronological control of the core is based on 22 ^{14}C AMS dates of selected plant macrofossils, following the protocols developed by Kilian et al. (1995) and Mauquoy et al. (2004). The selection of aboveground plant macrofossils ensures that accurate dates are assigned (*i.e.* free of rootlets and therefore of contamination). These macrofossils mainly consisted of *Sphagnum* spp. stems and opercula. In seven samples, *C. vulgaris* stems and/or *E. tetralix* stems and seed boxes were selected as the amount of *Sphagnum* spp. was not sufficient to provide large enough samples for dating. All samples were prepared at the GADAM Centre (Gliwice, Poland) using acid–alkali–acid washing (to remove any carbonate, bacterial CO_2 and humic/fulvic acid), drying and graphitisation following Goslar and Czernik (2000). Samples were measured at the Poznan radiocarbon Laboratory (Poznan, Poland) following the protocol from Goslar et al. (2004) and at the Rafter Radiocarbon Laboratory (Lower Hutt, New Zealand) following Zonderyan et al. (2007). Results are reported in Table 1. Lead 210 was also measured in recent layers (down to 18 cm depth) after ^{210}Po extraction from 2 g of dry peat powder spiked with ^{208}Po using a sequential HF-HNO_3–HCl digestion after peat ashing (De Vleeschouwer et al., 2010). Measurements were performed using an α-spectrometer (Canberra model 7401) for two days for each sample in order to obtain sufficient accuracy. The results of the calculation were corrected for the radioactive decay of ^{208}Po since the moment of its calibration, and the decay of ^{210}Pb since the moment of polonium extraction from the sediment. More details about the ^{210}Pb measurements at the GADAM Centre (Gliwice, Poland) can be found in Sikorski and Bluszcz (2008 and references therein). The Constant Rate of Supply (CRS) model (Appleby, 2001) was then applied in order to build the ^{210}Pb age-model. Uncertainties were calculated using the propagation of errors technique according to ISO GUM (Guide to the expression of Uncertainty in Measurement, www.iso.org). The modelled ages are reported in Table 2. The raw data, including background measurements of deeper samples, are reported in De Vleeschouwer et al. (2010).

3.3. Bulk density, Ti content

Samples were first freeze-dried following the protocol described in Le Roux and De Vleeschouwer (2010). To enable the volume-measurement of each slice, bulk density sub-samples were based on a c. 4 cm base × 4 cm height triangle cut out of each frozen slice (see Section 3.1). The dimension of each frozen triangle (including thickness) was measured to estimate the volume. The bulk dry density was calculated by weighing each sub-sample after water-removal by freeze-drying and by dividing its weight by its

Table 1
Radiocarbon sample type and results.

Depth (cm)	*Sphagnum* spp.			*Calluna vulgaris*		*Erica tetralix*		Age	Error	Lab. Code
	Stem	Branches + leaves	Capitulum	Branch	Leaf	Branch	Seed box	Uncal BP	*y*	
12.3	1				1		1	185	30	GdA-1380
28.1	9		20				2	215	30	GdA-1383
29.4	13							425	30	GdA-1620
30.7	15							450	30	GdA-1509
33.3	15							490	45	GdA-1510
35.8	10	10						460	30	GdA-1621
37.1				4				430	35	GdA-1622
38.3	20							620	30	GdA-1623
39.6	20							645	30	GdA-1624
40.8	25		2					355	30	GdA-1381
42.1								700	30	GdA-1427
43.4	15		3					650	40	GdA-1382
46.2	2		3	13		2	2	805	35	GdA-1384
47.6	21		7					840	30	GdA-1385
49.1	17		5					880	30	GdA-1388
57.2								935	30	GdA-1428
57.2	22		28					900	30	GdA-1386
67	32		4	1	1			1110	40	GdA-1387
75.5	1		10	1	5		5	1280	40	GdA-1389
78.3	25		14	1	2		1	1290	30	GdA-1390
86.8	7		16	8	1		1	1345	30	GdA-1391
99.4	31		15	3	0		2	1530	35	GdA-1392

Table 2
Lead 210 modelled ages for each sample down to 17.5 cm. Raw data (*i.e.* ^{210}Pb activities) are published elsewhere (De Vleeschouwer et al., 2010).

Depth (cm)	Top Age (AD)	Uncertainty (y)
0.97	2006	2
2.64	2005	2
3.8	2003	2
4.86	2002	2
5.98	2001	2
7.19	1999	2
8.45	1994	2
9.72	1990	2
11	1980	2
12.3	1969	3
13.7	1952	4
15	1930	5
16.3	1912	7
17.5	1745	9

volume. They were subsequently ground using a Retsch Mixer Mill, agate balls and plastic vials, prior to their chemical analyses.

The Ti content was measured on 1 g of dried and homogenised peat powder using a Brüker S8-Tiger wavelength-dispersive X-Ray Fluorescence (XRF) analyzer. The powder was analysed in 40 mm diameter plastic cups, with a 2.5-μm mylar film at the base. The XRF was calibrated with 27 certified reference materials, mostly consisting of organic matrices such as plant leaves, lichens, peat, organic sediments and coals (NIST-1515, 1547, 1570a, 1573a, 1575a, 1632b, 1635, 2718, 8437, 8438; BCR-60, 62, 129, 482; NIMT-UOE-FM-001; NIES-1, 3, 7, 8, 9, 10a, 10b, 10c; SARM-20; NJV-942 and 943). The detection limits was 2 μg g^{-1} while the standard deviations was 23 μg g^{-1}. Results are reported in Table 3.

3.4. Plant macrofossils

Plant macrofossil samples from MIS-8-06W were boiled with 5% KOH and sieved (mesh diameter 125 μm). Macrofossils were scanned using a binocular microscope (× 10–50), and identified using an extensive reference collection of type material (Mauquoy and van Geel, 2007). Volume percentages were estimated for all components with the exception of seeds, *Eriophorum vaginatum* spindles, *Sphagnum* spore capsules, and charcoal particles, which were counted and expressed as the number (*n*) present in each subsample. Zonation of the macrofossil diagrams was made using psimpoll 4.25 (optimal splitting by information content).

3.5. Pollen analyses

In order to distinguish between human and climate impacts in the record, several samples were studied for their arboreal and selected non-arboreal pollen content. For each sample, 2 g of fresh material was dissolved in 10% HCl after the addition of exotic *Lycopodium* spp. tablets for quantification. Treatment with KOH was omitted as this may damage pollen microfossils in addition to the added *Lycopodium* spores. The residues were then dissolved in 96% acetic acid and treated by acetolysis. After centrifugation, the solutions were filtered through 200 μm and 12 μm mesh sieves. The residues were washed in 96% alcohol and transferred in glycerin to be mounted on glass slides.

3.6. Stable isotopes

3.6.1. Specimen selection

Two types of specimen were selected: species/section specific *Sphagnum* macrofossils and *Sphagnum* spp. debris.

For species/section specific *Sphagnum,* stems of *Sphagnum imbricatum* (42 samples) and *Sphagnum papillosum* (9 samples), in addition to stems of *Sphagnum* section *Cuspidata* (7 samples) were collected using watchmakers forceps from samples which had first been treated with 5% KOH, sieved and rinsed with distilled water. Following the recommendations of Loader et al. (2007) only stems were selected and where necessary, any attached leaves were removed. The stems were placed into sealed phials.

To separate species/section specific *Sphagnum* debris from the peat, each sample was successively sieved through 2000, 630, 355, and 200 μm mesh sizes with a minimum of 5 L of deionised water (Daley et al., 2010). Each size fraction was examined for its composition under a stereoscopic binocular microscope (Nikon SMZ 2B). The size fraction of 355–630 μm has been identified to almost exclusively consist of *Sphagnum* spp. leaves. Therefore, this size fraction was used for cellulose extraction and stable isotope measurement. Cellulose extraction from the individual samples followed an improved extraction method based on sample bleaching with sodium chlorite (Ménot and Burns, 2001), followed by cellulose dissolution in cuprammonium solution ($[Cu(NH_3)_4](OH)_2$) and re-precipitation using sulphuric acid (Wissel et al., 2008). This approach achieves pristine cellulose not by removing any contaminants from the cellulose, but by dissolving the cellulose from bulk organic matter. This way, contaminations of *Sphagnum* spp. cellulose with small amounts of minerogenic matter like silt and clay and/or biogenic opal could be completely excluded. The obtained cellulose was highly homogeneous, ensuring isotopic homogeneity when using small sample amounts for isotope measurements.

3.6.2. Analytical methods

Stable carbon isotope analyses were carried on two types of specimen: 1) species/section specific *Sphagnum* stems and 2) *Sphagnum* cellulose from the sieve fraction of 355–360 μm (*Sphagnum* spp. leaves). Oxygen isotope analyses were performed on only the second type of specimen.

The stable carbon isotope measurements of species/section specific *Sphagnum* stems were undertaken on bulk plant material, because separation of an adequate amount of stems for cellulose extraction was too time consuming and not possible for each sample.

The stable carbon isotope measurements of both species/section specific *Sphagnum* stems and *Sphagnum* cellulose were measured by online combustion of *c.* 30 μg dry stems and 200–300 μg dry cellulose, respectively. Samples were weighed into tin foil cups and combusted at 1080 °C using an EuroEA elemental analyser (Euro Vector Instruments, Italy) to generate CO_2 for an interfaced IsoPrime continuous flow isotope ratio mass spectrometer (GV Instruments, United Kingdom). Each sample was measured once and approximately every eleventh sample was measured twice to check reproducibility. For species/section specific *Sphagnum* stems, each sample was measured in triplicate to check the reproducibility.

Oxygen isotope ratios of *Sphagnum* cellulose were measured by online combustion of 275 ± 20 μg dry cellulose weighed into silver foil cups, which were then vacuum-dried and subsequently pyrolysed at 1450 °C using a high temperature pyrolysis analyser (HT-O, HEKAtech, Germany) to generate CO for the same interfaced IRMS. For the determination of oxygen isotopes, each sample was measured at least three times.

Results are reported using the conventional δ-notation in per mill vs. V-PDB for carbon and V-SMOW for oxygen. USGS24 graphite and IAEA-C3 cellulose were used as certified reference materials. The overall precision of replicate analyses of samples is estimated to be better than ±0.22‰ and ±0.1‰ for $\delta^{13}C_{stem}$ and $\delta^{13}C_{cell}$, respectively and better than ±0.3‰ for $\delta^{13}O_{cell}$ (1σ).

Table 3
Bulk density, Ti content, stable carbon and oxygen results of the peat core.

Mid-point depth (cm)	Density (g cm^{-3})	Ti (μg g^{-1})	Species/section used for $\delta^{13}C_{stem}$	$\delta^{13}C_{stem}$ vs. V-PDB (‰)	$\delta^{13}C_{stem}$ vs. V-PDB standard deviation (‰)	$\delta^{13}C_{cell}$ vs. V-PDB (‰)	$\delta^{13}C_{cell}$ vs. V-PDB standard deviation (‰)	$\delta^{18}O_{cell}$ vs. SMOW (‰)	$\delta^{18}O_{cell}$ vs. SMOW standard deviation (‰)
0.97		261				−21.59	0.06	28.23	0.06
2.64	0.019	18				−25.08	0.20	25.23	0.20
3.80	0.016	17	*S. papillosum* stems	−27.58	0.14	−24.56	0.28	25.18	0.28
4.86	0.015	8	*S. papillosum* stems	−28.24	0.13	−23.82	0.11	25.23	0.11
5.98	0.022	63	*S. papillosum* stems	−27.58	0.30	−25.37	0.28	25.18	0.28
7.19	0.065	164	*S. papillosum* stems	−26.98	0.14	−25.48	0.38	24.93	0.38
8.45	0.046	183	*S. papillosum* stems	−28.21	0.15	−26.07	0.10	25.07	0.10
9.72	0.109	617	*S. papillosum* stems	−27.57	0.13	−23.23	0.35	28.85	0.35
11.0	0.091	509				−23.57	0.10	26.49	0.10
12.3	0.145	638				−23.46	0.10	27.01	0.10
13.7	0.154	552	*S. imbricatum* stems	−27.26	0.14	−22.54	0.42	29.16	0.42
15.0	0.144	455				−22.95	0.27	27.99	0.27
16.3	0.112	269	*S. imbricatum* stems	−26.67	0.30	−23.67	0.17	26.80	0.17
17.5	0.094	220	*S. imbricatum* stems	−28.03	0.30	−23.48	0.25	26.70	0.25
18.8	0.074	194	*S. imbricatum* stems	−25.78	0.15	−24.30	0.39	26.55	0.39
20.2	0.096	239	*S. imbricatum* stems	−27.78	0.13	−23.49	0.02	27.34	0.02
21.5	0.078	209				−23.35	0.09	26.84	0.09
22.9	0.108	216	*S. imbricatum* stems	−26.26	0.13	−22.99	0.06	27.95	0.06
24.2	0.124	216	*S. imbricatum* stems	−27.43	0.15	−23.78	0.06	27.70	0.06
25.5	0.112	204	*S. imbricatum* stems	−29.59	0.30	−23.28	0.10	27.13	0.10
26.7	0.130	210	*S. papillosum* stems	−26.18	0.15	−23.24	0.05	27.47	0.05
28.1	0.109	196	*S. imbricatum* stems	−24.90	0.13	−23.07	0.43	26.48	0.43
29.4	0.080	185	*S. papillosum* stems	−25.14	0.14	−23.16	0.29	26.90	0.29
30.7	0.102	174							
32.0	0.088	236				−23.81	0.04	26.46	0.04
33.3	0.101	280	*S. imbricatum* stems	−26.87	0.15	−23.24	0.28	26.87	0.28
34.5	0.098	216	*S. imbricatum* stems	−24.70	0.13	−23.75	0.09	27.68	0.09
35.8	0.093	283	*S. imbricatum* stems	−26.44	0.13	−23.52	0.01	27.61	0.01
37.1	0.093	237				−23.44	0.32	26.91	0.32
38.3	0.082	201	*S. imbricatum* stems	−26.80	0.15	−22.30	0.33	26.52	0.33
39.6	0.073	144				−22.96	0.09	27.32	0.09
40.8	0.072	284	*S. imbricatum* stems	−26.45	0.30	−21.71	0.22	26.54	0.22
42.1	0.078	279	*S. imbricatum* stems	−26.06	0.14	−21.91	0.11	26.63	0.11
43.4	0.065	262	*S. imbricatum* stems	−25.90	0.30	−23.62	0.03	24.80	0.03
44.8	0.067	140	*S.* s. *Cuspidata* stems	−26.00	0.30	−23.50	0.14	23.55	0.14
46.2	0.074	179	*S.* s. *Cuspidata* stems	−26.35	0.14	−22.82	0.04	24.58	0.04
47.6	0.059	142	*S.* s. *Cuspidata* stems	−29.50	0.30	−22.62	0.08	25.40	0.08
49.1	0.092	321	*S. imbricatum* stems	−27.65	0.13	−23.86	0.19	27.18	0.19
50.5	0.075	136	*S. imbricatum* stems	−27.51	0.14	−23.35	0.42	26.01	0.42
51.8	0.054	113	*S. imbricatum* stems	−26.33	0.14	−22.79	0.09	26.97	0.09
53.1	0.046	81	*S. imbricatum* stems	−25.83	0.14	−23.05	0.55	26.70	0.55
54.4	0.050	42	*S. imbricatum* stems	−27.80	0.14	−22.29	0.06	26.22	0.06
55.8	0.043	36	*S. imbricatum* stems	−27.58	0.15	−22.24	0.20	25.90	0.20
57.2	0.085	164	*S. imbricatum* stems	−25.80	0.13	−23.23	0.17	27.39	0.17
58.5	0.045	121	*S. imbricatum* stems	−30.55	0.13	−23.29	0.21	26.42	0.21
59.7	0.048	90							
60.9	0.052	60	*S. imbricatum* stems	−27.43	0.14	−24.11	0.13	26.35	0.13
62.2	0.075	207	*S. imbricatum* stems	−27.87	0.13	−23.27	0.22	27.08	0.22
63.5	0.061	105	*S. imbricatum* stems	−27.17	0.13	−23.49	0.20	26.94	0.20
64.7	0.058	37	*S. imbricatum* stems	−28.71	0.15	−23.94	0.17	26.50	0.17
65.8	0.060	52	*S. imbricatum* stems	−27.08	0.13	−23.20	0.40	26.70	0.40
67.0	0.059	87	*S.* s. *Cuspidata* stems	−25.53	0.30	−23.15	0.14	26.01	0.14
68.4	0.077	96				−22.76	0.10	26.47	0.10
69.8	0.078	87				−21.58	0.02	26.20	0.02
71.1	0.071	88							
72.5	0.064	88	*S.* s. *Cuspidata* stems	−18.68	0.13	−17.82	0.16	24.72	0.16
74.1	0.076	56	*S.* s. *Cuspidata* stems	−19.05	0.14	−18.42	0.25	24.03	0.25
75.5	0.075	161	*S.* s. *Cuspidata* stems	−19.96	0.13	−21.73	0.05	26.26	0.05
76.9	0.076	175	*S. imbricatum* stems	−20.62	0.15	−22.28	0.24	26.03	0.24
78.3	0.084	120	*S. imbricatum* stems	−24.30	0.30	−22.82	0.08	26.32	0.08
79.7	0.078	86	*S. imbricatum* stems	−24.84	0.30	−22.76	0.21	26.28	0.21
81.2	0.040	11	*S. imbricatum* stems	−26.05	0.13	−22.78	0.03	27.00	0.03
82.6	0.045	9	*S. imbricatum* stems	−28.05	0.14	−22.80	0.09	26.08	0.09
84.1	0.057	19	*S. imbricatum* stems	−28.86	0.30	−23.20	0.26	25.65	0.26
85.4	0.078	50	*S. imbricatum* stems	−28.82	0.15	−23.25	0.33	26.16	0.33
86.8	0.081	71				−23.63	0.20	27.04	0.20
88.2	0.088	83	*S. imbricatum* stems	−27.43	0.14	−23.68	0.60	26.37	0.60
89.6	0.085	79	*S. imbricatum* stems	−27.42	0.14	−23.34	0.16	26.71	0.16
91.0	0.073	65	*S. imbricatum* stems	−26.00	0.30	−23.25	0.18	26.35	0.18
92.3	0.057	45	*S. imbricatum* stems	−27.86	0.15	−23.26	0.11	26.53	0.11
93.7	0.077	77				−24.05	0.26	26.22	0.26
95.1	0.058	22	*S. imbricatum* stems	−26.44	0.13	−23.16	0.25	26.15	0.25
96.4	0.057	19	*S. imbricatum* stems	−26.26	0.14	−22.94	0.25	25.79	0.25
97.9	0.054	33	*S. imbricatum* stems	−27.17	0.15	−23.48	0.49	26.63	0.49
99.4	0.067	46				−23.85	0.36	26.17	0.36

Coal, oil and gas are of organic origin and thus depleted in ^{13}C. Anthropogenic fossil fuel burning, which increased the concentration of atmospheric CO_2, lowered the $\delta^{13}C$ value of air by about 1.7‰ since the onset of industrialisation. Therefore, all *Sphagnum* $\delta^{13}C_{cellulose}$ values of post-1850 AD samples were corrected by adding a $\delta^{13}C$ correction factor interpolated from measured and estimated annual data (Leuenberger, 2007). Results are reported in Table 3.

3.7. Data comparison

In order to compare macrofossil results and stable isotope results, two statistical tests were performed, as described below. Prior to analysis, the data were checked for normality, but even after transformation (log and square root) a Kolmogorov–Smirnov test confirmed that the distributions were significantly not normally distributed. The effect of species/section composition of *Sphagnum* was therefore first explored using the Kruskal–Wallis test (test statistic H), and post hoc tests were conducted using the Mann–Whitney test (test statistic U). Both tests were undertaken using SPSS v.17 software. Partial correlations were also calculated between standardised values of the DCA axis 1 scores, $\delta^{13}C$ of *Sphagnum* cellulose, and $\delta^{13}C$ of *Sphagnum* species/section specific stems.

4. Results and discussion

4.1. Chronology and accumulation rates

An age-model was constructed using the ^{14}C dates and the CRS modelled ^{210}Pb ages. Radiocarbon dates were translated to calendar distributions using the IntCal09 calibration curve (Reimer et al., 2009). Through the dated depths, age-depth models were drawn consisting of 50 1-cm thick sections of piece-wise linear accumulation, with the accumulation rate of each section depending somewhat on the previous section (an autoregressive process with a degree of "memory") (Blaauw et al., 2011). This process resembles the Bpeat routine of Blaauw and Christen (2005), although it uses many more sections and thus results in more flexible age-depth models. Using an iterative Markov Chain Monte Carlo process, several thousands of independent likely age-depth models were constructed, each of them assigning calendar ages to all depths (dated or non-dated). From these models, calendar age distributions were constructed for all depths, and depicted as grey-scales where more likely calendar ages are depicted by darker grey levels (Fig. 2). Less secure sections of the age-depth model are indicated by lighter grey spread over larger areas. The same age-models can be used to produce grey-scale plots of proxy values (see discussion and Fig. 6a–b), where the calendar scale uncertainties are also indicated using grey-scales (Blaauw et al., 2007).

From the base (*ca.* 500 AD) of the peat profile towards 25.5 cm (around 1600 AD), the mean peat accumulation rate continuously decreases from *c.* 1 mm y^{-1}, to 0.32 mm y^{-1}. In the first half of the profile however, the peat accumulation rate peaks around 600–670 AD (1.4 mm y^{-1}), 690–850 AD (1.6 mm y^{-1}), 870–1030 AD (1.1 mm y^{-1}) and 1130–1200 AD (0.9 mm y^{-1}). Above 25.5 cm, and until the top, the accumulation rate increases drastically and marks the progressive shift from the catotelm to the acrotelm, characterised by living plants and uncompressed peat.

4.2. Palaeoenvironmental, palaeoclimatic and human indicators

4.2.1. Pollen evidence of human impact and possible climatic changes

The lower part of the pollen diagram (99.4 cm–53.1 cm), where *Fagus* is equal to or higher than 20% (Fig. 3), belongs to Zone IX as defined by Firbas (1949). However, the *Fagus* curve is strongly influenced by abundances of *Alnus* and, to a lesser extent, by *Betula*, two species growing on the bog (assuming *Betula* may be *Betula pubescens*). Above, the Zone X of Firbas (1949) starts with a clear increase of *Quercus* and a subsequent decrease of *Fagus.*

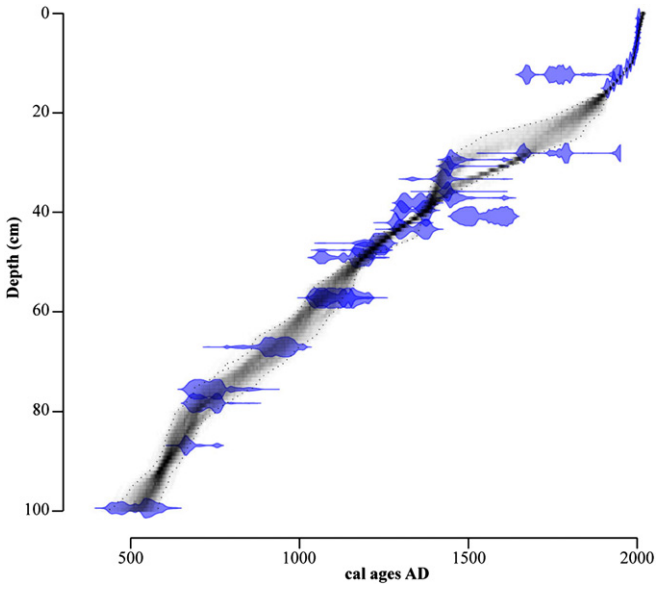

Fig. 2. Age-model produced by BACON software (Blaauw et al., 2011) coupling both ^{14}C and ^{210}Pb results. Age-models are based on 50 1-cm thick sections of linear accumulation, with a degree of memory between each section. Grey-scales indicate all likely age-depth models, and dotted lines indicate the 95% confidence ranges. Shapes show calendar age distributions of individual dates (calibrated distributions for the ^{14}C dates).

Here, a subdivision of Zones IX and X based on tree ecology is attempted. Zones 1 and 2 have high values (>5%) of *Carpinus*. In zone 1, *Alnus* is also commonly more abundant than *Betula*, indicating a more humid climate than in zone 2. In Zone 3, *Fagus* and *Quercus* relative abundances oscillate between 15% and 30%, with a general slow decreasing trend of *Fagus* values. These values are however strongly dependent upon the important values of *Betula* and its possible species. *Betula pendula* is abundant on relatively dry acidic soils, whereas *B. pubescens* may expand on the bog during periods of low *Sphagnum* abundance. Therefore, Zone 3 may correspond to the drier climatic conditions of the Medieval Warm Period (MWP). *Quercus* values clearly increase above *Fagus* values during the transition from Zones 3 to 4, and clearly dominate in Zone 4. The dominance of *Quercus* may be partly explained by the fact that it is used as cattle fodder, whereas its bark and wood were intensively used. On the other hand, *Fagus* is not only unable to survive wood fires, but is also strongly influenced by regular cutting to produce charcoal. This industry is known from the XVIth century in the Rurbusch forest, a few km to the south of the Misten bog (Liégeois-Lemaitre, 1957). *Fagus* cannot therefore compete with other trees such as *Quercus,* which regenerates more easily from stumps. The rise of *Pinus sylvestris* up to *c.* 10% in the upper half of Zone 4 may correspond to its first introduction in the nearby forest *Hertogenwald* (near Eupen) around 1750 (Pahaut and Oldenhove de Guertechin, 1962). Zone 5 (second half of the XIXth century) is characterised by a significant increase of *P. sylvestris* and the occurrence of *Picea abies*, both species having been extensively planted in the area. The main changes in *Poaceae* and *Cerealia* curves occur in the transition from Zone 2 to Zone 3, where their respective abundances remain generally below 10% and 6%. *Cerealia* peaks (>10%) in Zone 4, while *Poaceae* maximum abundances (>30%) are found in Zone 5. *Plantago* (mainly *Plantago lanceolata*)

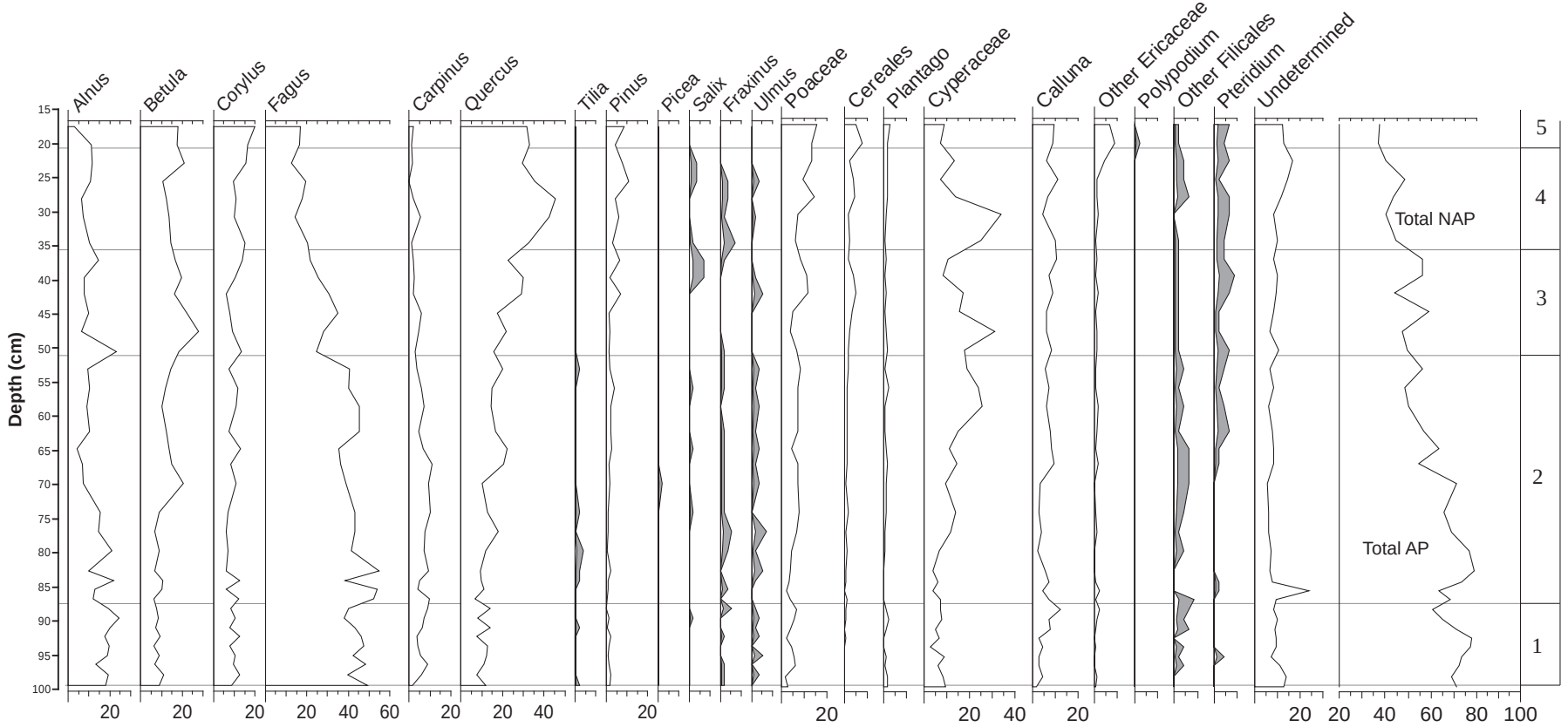

Fig. 3. Relative arboreal and selected non-arboreal pollen abundances (%) in the Misten peat profile. Grey areas are ×4 exaggerations for selected low pollen content.

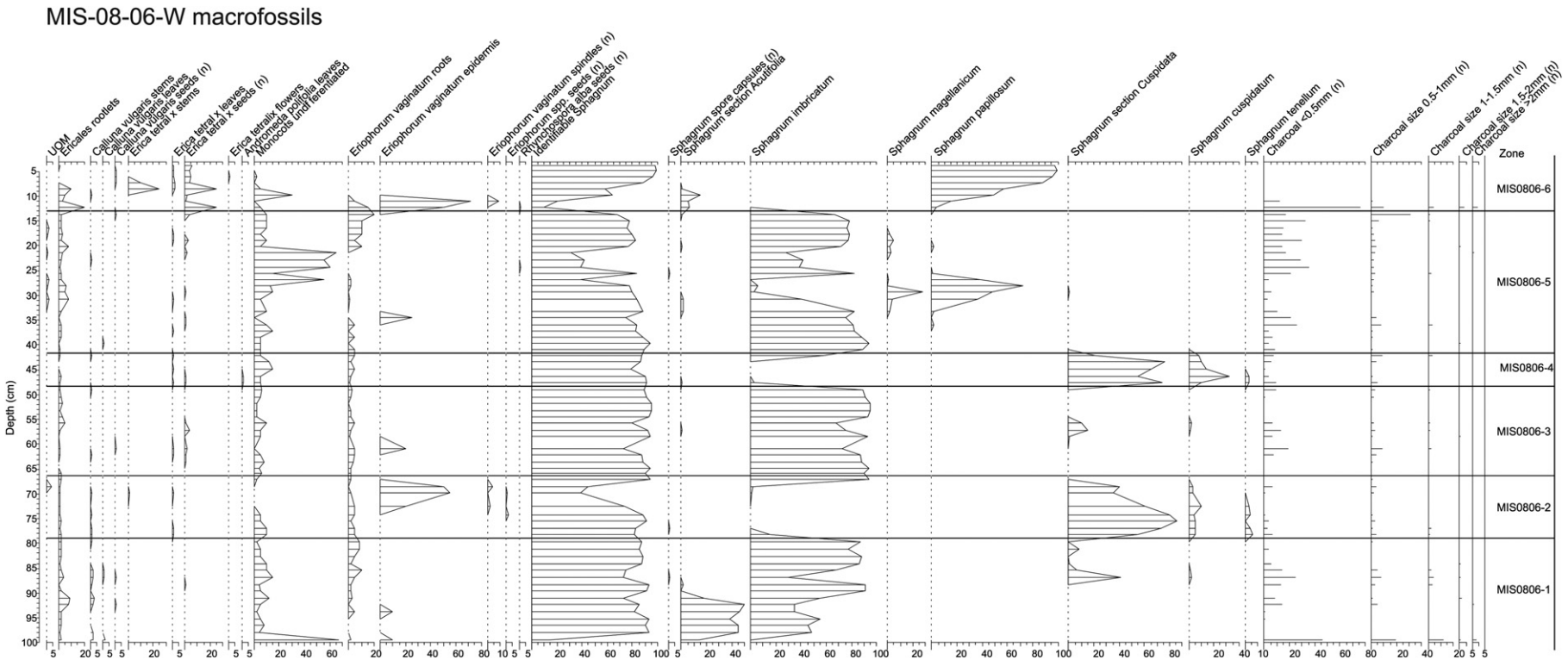

Fig. 4. Plant macrofossil diagram of MIS-08-06W. Volume abundances of all components are expressed as percentages with the exception of seeds, *Eriophorum vaginatum* spindles, *Sphagnum* spore capsules, *Cenococcum* sclerotia, *Meliola ellisii* (Type 14) fruit-bodies and charcoal particles, which were counted and expressed as the number (*n*) present in each ~5 cm^3 sub-sample.

Table 4
Macrofossil zonation and main features.

Macrofossil zone	Depth (cm)	Main features
MIS-08-06W-6	13–0	Following peat charcoal abundance at 12.3 cm, this declines then reduces to zero. Initially abundant *Eriophorum vaginatum* epidermis is replaced by *Sphagnum papillosum*. Peak values of *Erica tetralix* stems and seeds occur in this zone.
MIS-08-06W-5	41.4–13	Initial high values of *Sphagnum imbricatum* are followed by high abundances of *Sphagnum papillosum* with the first appearance of *Sphagnum magellanicum* between 33.3 and 26.7 cm. Monocots undifferentiated and *Sphagnum imbricatum* then alternate as the predominant components of the peat matrices. Marked increase in the number of charcoal fragments.
MIS-08-06W-4	48.4–41.4	Second phase of abundant *Sphagnum* section *Cuspidata* leaves with peak recorded values of *Sphagnum cuspidatum*.
MIS-08-06W-3	67.7–48.4	Marked increase of *Sphagnum imbricatum* which records high abundances throughout. Moderate increase in charcoal and a minor presence of *Sphagnum* section *Cuspidata* leaves between 57.2 and 55.8 cm
MIS-08-06W-2	79–67.7	Abundant *Sphagnum* section *Cuspidata* leaves followed by abundant *Eriophorum vaginatum* epidermis. Reduced charcoal present.
MIS-08-06W-1	99.4–79	Abundant *Sphagnum* section *Acutifolia* leaves are replaced by abundant *Sphagnum imbricatum* leaves at 89.6 cm. A peak of *Sphagnum* section *Cuspidata* leaves occurs at 86.8 cm. Relatively high values of charcoal are recorded between 92.3 and 85.4 cm.

abundance peaks in Zone 5. As it mainly characterises wet meadows and pastures rather than cultivation, *Plantago* may reflect agricultural changes toward a cattle-based economy on meadows in the area. Cyperaceae (*Eriophorum*) develops in Zone 2 and is replaced by *Calluna* and other Ericaceae from the upper part of Zone 4 to Zone 5. This characteristic may indicate a drying of the uppermost peat layers. However *Calluna* and other Ericaceae are also characteristic of wet and dry heath land. Unless the *Calluna* and other Ericaceae values are very high, it is therefore difficult to recognize the source area of these species.

4.2.2. Macrofossil evidence for changes in mire surface wetness

The results of the plant macrofossil analyses are presented in Fig. 4. The main features of the zones are described in Table 4. In zones MIS-08-06-2 and MIS-08-06-4 increases in mire surface wetness were recorded between 79–68 cm and 48–41 cm. Detrended Correspondence Analysis (DCA) was used to explore the presence of a mire surface wetness gradient in the plant macrofossil data using CANOCO 4.5 (detrending by segments, no transformation and down-weighting of rare species). The DCA ordination is presented in Fig. 5. The gradient length of axis 1 is 3.564 and accounts for 28.4% of the variance of the species data. There is a separation between the wet/dry macrofossil components, and evidence for a water level gradient along DCA axis 1. Hygrophilous mire taxa (*Sphagnum* section *Cuspidata*, *Sphagnum cuspidatum*, and *Sphagnum tenellum*) have high eigenvalues, whereas 'drier' indicator species (Ericaceae rootlets and *Sphagnum* section *Acutifolia*) have relatively lower values.

4.2.3. Stable isotope signature

The oxygen isotope composition of *Sphagnum* cellulose ($\delta^{18}O_{cell}$) in combination with the stable carbon isotope composition of *Sphagnum* cellulose ($\delta^{13}C_{cell}$) and the species/section specific *Sphagnum* stems ($\delta^{13}C_{stem}$) are presented in Fig. 6a.

In general, the oxygen isotopic composition of cellulose from terrestrial plants depends on: 1) the isotopic composition of the plant's source water, 2) the enrichment of heavier isotopes in leaf water due to evapotranspiration and 3) the overall biochemical fractionation between source water and cellulose (DeNiro and Epstein, 1979, 1981; Sternberg et al., 1986). Due to the considerably larger surface of relatively dry hummocks compared to wet hollows and open pools, evaporation is much higher above *Sphagnum*-covered hummocks than above hollows and pools. The $\delta^{18}O_{water}$ in hummocks is therefore significantly more enriched in ^{18}O than in hollows or pools (Ménot-Combes et al., 2002). Another explanation for this difference may be found in heat transfer variations. The water thermal conductivity coefficient ranges from 0.597 W mK^{-1} at 283 K to 0.61 W mK^{-1} at 293 K (Martin and Lang, 1933). However, the thermal conductivity coefficient for living *Sphagnum* mosses varies from *c.* 0.030 W mK^{-1} for dry plants to *c.* 0.55 W mK^{-1} for plants containing about 90% of volumetric water (O'Donnell et al., 2009). Therefore, differences of heat transfer coefficients may also cause differences in evapotranspiration rates in dry hummocks and wet hollows and pools. The solar energy delivered to the water in the pools and very wet plants will be easily transferred, while the same energy delivered into small residual water volumes of the living plants will increase energy of the water molecules to the level necessary for evaporation.

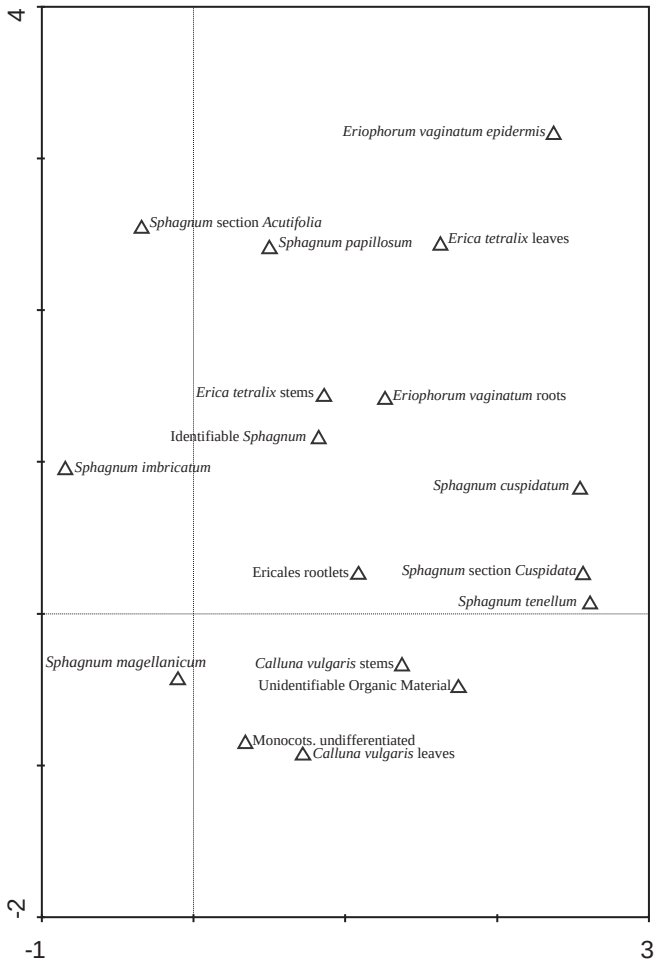

Fig. 5. DCA ordination performed on the macrofossil dataset.

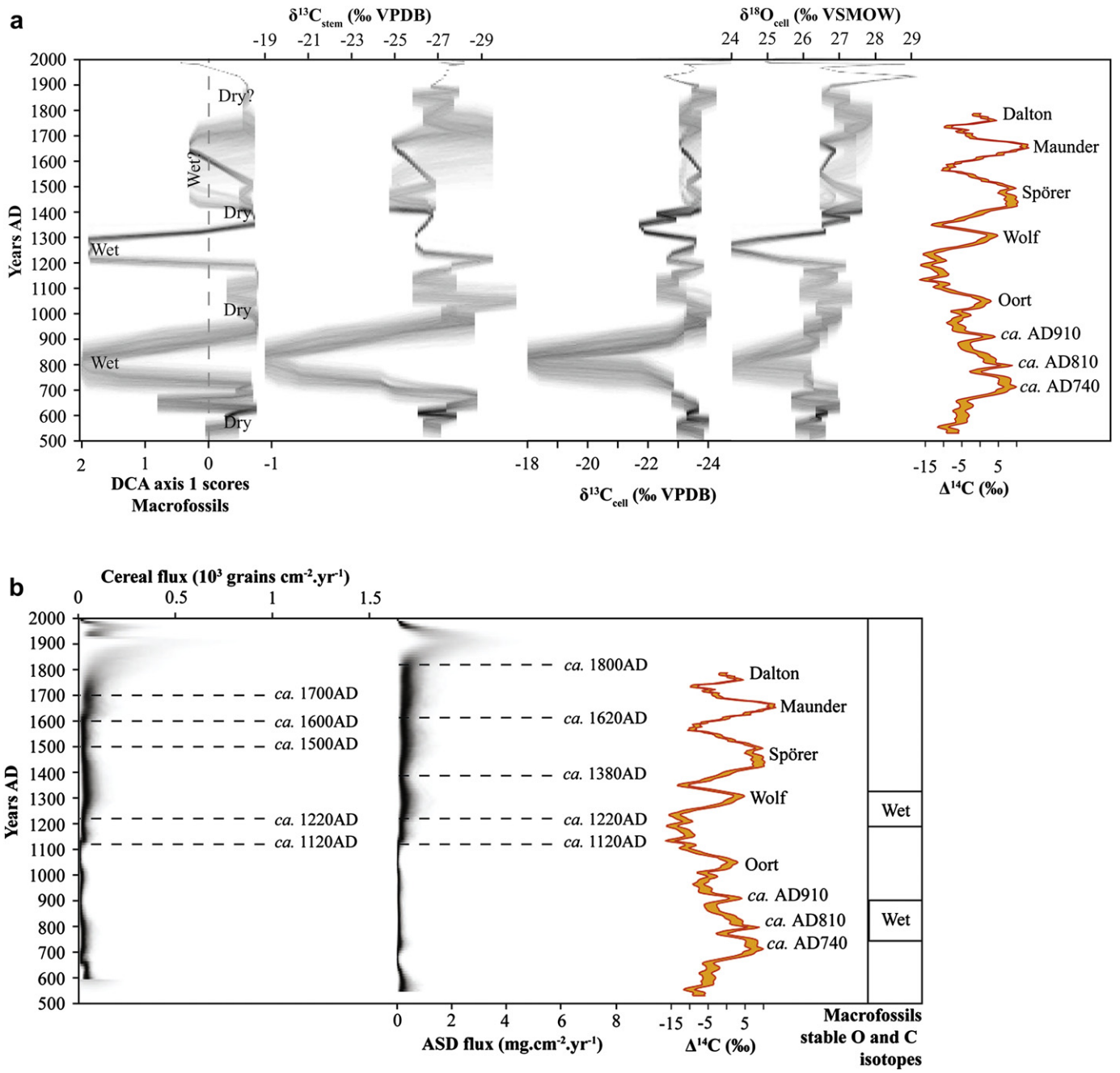

Fig. 6. (a) DCA axis score 1 of the macrofossil data, $\delta^{13}C_{cell}$, $\delta^{13}C_{stem}$ and $\delta^{13}O_{cell}$ values and comparison with the $\Delta^{14}C$ curve from Reimer et al. (2009). (b) ASD and Cereals fluxes compared to the $\Delta^{14}C$ curve from Reimer et al. (2009) and wet phases recorded by macrofossils and stable C–O isotopes. Dashed lines symbolize age boundaries between two periods of enhanced flux.

As a consequence of both possibilities, the $\delta^{18}O_{cell}$ time series should provide an indication of past micro-habitat conditions in fens and mires.

At the Misten bog, the $\delta^{18}O_{cell}$ measurements record large variability. Two pronounced excursions towards significantly reduced $\delta^{18}O_{cell}$ values occur during the 8th–9th and 13th centuries. The ^{18}O-depleted values presumably indicate phases of reduced evaporation and are therefore interpreted as 'shallow pool phases' with relatively low evaporative enrichment of the heavier oxygen isotope, resulting in depleted $\delta^{18}O_{water}$ and thus also in depleted $\delta^{18}O_{cell}$ values. Compared to these two hollow or even pool micro-habitat phases, the rest of the $\delta^{18}O_{cell}$ record points to a drier mire microtopography, with higher evaporative enrichment of the bog surface water from a hummock-like surface.

The two large shifts to depleted $\delta^{18}O_{cell}$ values coincide with the replacement of *S. imbricatum* (the dominant species for the last *ca.* 1500 years) by *Sphagnum* section *Cuspidata* (Fig. 4). The occurrence of *Sphagnum* section *Cuspidata* is restricted to wet bog surface conditions since this species is mostly found in wet hollows and shallow pools (Barber and Langdon, 2007). The wet/dry bog surface conditions indicated by the $\delta^{18}O_{cell}$ data are therefore in good agreement with the macrofossil interpretations. $\delta^{18}O_{cell}$ wet phases occur in macrofossil Zones 2 and 4, while $\delta^{18}O_{cell}$ dry phases occur in macrofossil Zones 1, 3 and 5.

The overall value of the enrichment factor between the oxygen isotope composition of source water and moss cellulose ($\Delta_{cell-water}$) from recent bog habitats has been found to be species dependent (Ménot-Combes et al., 2002). Habitat conditions also play a significant role since hollow species, such as *Sphagnum* section *Cuspidata*, have been found to provide more constant $\Delta_{cell-water}$ values than more drought-resistant hummock species, thus yielding large variability in their $\delta^{18}O_{cell}$ values (Ménot-Combes et al., 2002; Zanazzi and Mora, 2005). Therefore, the $\delta^{18}O_{cell}$ time series found in the Misten bog record high variability ($\sim$5.6‰), with oxygen isotope values ranging from 23.6 to 29.2‰ (Fig. 6a). Approximately half of this variability can be explained by the two 'shallow pool phases' with substantially depleted $\delta^{18}O_{cell}$ values during the 8th–9th and the 13th centuries. Additionally, during the 20th century, the variability in the $\delta^{18}O_{cell}$ times series is comparatively high and most likely caused by massive human impact on the hydrological conditions at Misten bog (see Section 2 and Hindryckx and Streel, 2000).

Even if the two 'shallow pool phases' and the high $\delta^{18}O_{cell}$ variability during the second half of the 20th century are not taken into account, the $\delta^{18}O_{cell}$ values of *Sphagnum* plant material growing on a hummock record relatively high variability. Large uncertainties associated with the $\delta^{18}O_{cell}/\delta^{18}O_{water}$ relationship for bog and mire ecosystems generally limit the use of the oxygen isotope composition of *Sphagnum* cellulose from peat deposits in palaeoclimate reconstruction (Zanazzi and Mora, 2005). Therefore only the pool phases can be interpreted with certitude in terms of changing hydrological conditions inducing shifts in the $\delta^{18}O_{cell}$ values of $\sim$3–4‰. This limits the ability to detect environmental and climate variability using the $\delta^{18}O_{cell}$ time series. Nevertheless there is much evidence for two distinct 'shallow pool phases' during the 8th to 9th and during the 13th century, and intermediate dry phases.

More comprehensive studies on the carbon isotopic composition of mosses and its relationship to climate provide evidence that the $\delta^{13}C_{cell}$ of moss cellulose reflects changes in bog and mire surface wetness (Price et al., 1997; Rice, 2000; Loisel et al., 2009). At the Misten bog, the $\delta^{13}C_{cell}$ values are on average significantly higher than the $\delta^{13}C_{stem}$ values, whereby the mean isotopic offset of *c.* 3.4‰ can be mainly attributed to two different reasons: (1) the stable carbon isotope composition of untreated *Sphagnum* plant material is in general lighter than the comparable cellulose values (Menot-Combes et al., 2001) and (2) there is a significant isotopic offset between *Sphagnum* stems and branches in modern but also fossil *Sphagnum* plant material (Loader et al., 2007; Moschen et al., 2009). Since (1) the sieved fraction of single leaves, which has been used for cellulose extraction, reflects the isotopic signal of *Sphagnum* branches and (2) the overall isotopic offset between untreated *Sphagnum* plant material and cellulose, the isotopic offset between $\delta^{13}C_{stem}$ and $\delta^{13}C_{cell}$ is easy to explain. Furthermore, because a limited sample amount was available for stable isotope investigations, the $\delta^{13}C_{stem}$ values were typically based on two to five single *Sphagnum* stems. *Sphagnum* stems from different plants of the same species growing at the same time have shown a stable carbon isotope signature varying by 2‰ or even more (Loader et al., 2007). Conversely, the $\delta^{13}C_{cell}$ values are based on samples containing several thousand single *Sphagnum* leaves grown throughout several growing seasons and thus are well homogenised and replicable (Moschen et al., 2009; Loisel et al., 2010). Problems associated with changes in the relative proportion of different physical plant or chemical compounds over time can thus be excluded in this type of analysis (Rinne et al., 2005). Therefore, it is expected that the $\delta^{13}C_{cell}$ values will better reflect changes in the bog surfaces wetness than will the $\delta^{13}C_{stem}$. Nevertheless, despite the much larger scatter of the $\delta^{13}C_{stem}$ time series, a large shift to ^{13}C-enriched values from *ca.* 700 AD to *ca.* 800 AD is clearly shown in both time series. It indicates that at Misten bog the $\delta^{13}C_{stem}$ is also effected by important environmental and climate variability.

The $\delta^{13}C_{cell}$ time series is interpreted to record the mire surface wetness at the Misten bog during the growing season. Thereby, it can be assumed that the *Sphagnum* $\delta^{13}C_{cell}$ values are weighted toward the spring and autumn months, because *Sphagnum* plants significantly reduces their rate of photosynthesis and thus their relative growth rate during the summer, when the bog surface wetness decreases (Williams and Flanagan, 1996; Rice, 2000). From *ca.* 500 AD to *ca.* 750 AD, the $\delta^{13}C_{cell}$ record shows relatively small fluctuations. A pronounced shift to ^{13}C-enriched values occurs during the 8th and 9th century, pointing to extremely wet conditions. Wet conditions during this time span were already suggested by the oxygen isotope composition of the *Sphagnum* cellulose and macrofossil distribution. Thus, there is much evidence, that during the 8th and 9th century, the area around the Misten bog was a wet and also, a cold environment.

A second peat unit (*ca.* 13th century) is also almost exclusively composed of *Sphagnum* section *Cuspidata* (Fig. 4), pointing to wet conditions. However, whereas both macrofossil and $\delta^{18}O_{cell}$ point towards wet conditions, the $\delta^{13}C_{cell}$ time series give no indication of such wet conditions during this phase. Since the stable carbon isotope signature of *Sphagnum* cellulose is more responsive to hydrological parameters and thus to environmental and climatic conditions rather than to species specific features (Loisel et al., 2009), the non-response of the $\delta^{13}C_{cell}$ time series during the 13th century in the Misten core is rather puzzling. The authors can only speculate that during the 13th century, the bog surface was not as wet as during the 8th to 9th century. That would imply that the species shift to *Sphagnum* section *Cuspidata* after *ca.* 1200 AD is a result of a rising water table, leading to a wetter peat, but not to a real pool development. The hydrological conditions would have not changed as much as during the 8th and 9th century, implying a growth of *Sphagnum* section *Cuspidata* under hollow conditions while under shallow pool conditions during the 8th to 9th century.

In contrast, an admixture of remains from higher plants to the sieved fraction of *Sphagnum* leaves which forms the basis of the $\delta^{13}C_{cell}$ record is unlikely to account for the massively ^{13}C-enriched values during the 8th and 9th century. Such an admixture would result in higher $\delta^{13}C$ values, since in bog and mire ecosystems

higher plants are in general more enriched in ^{13}C than mosses (Ménot and Burns, 2001). Since the $\delta^{13}C_{stem}$ time series, which is clearly attributable to pure *Sphagnum* plant material, also depict the large shift to ^{13}C-enriched values from *ca.* 700 AD to *ca.* 800 AD, such an admixture can, however, be excluded.

On the other hand, problems associated with the climatic significance of stable carbon isotope values from hollow and particularly pool species have been described (e.g. Ménot and Burns, 2001; Loisel et al., 2009). *Sphagnum* species growing on hummocks yield lighter $\delta^{13}C_{cell}$ values than hollow and pool species, because hummock species photosynthesise under lower water content and thus lower external diffusive resistance (Price et al., 1997). The $\delta^{13}C_{cell}$ ranges reported from recent mire surfaces are significantly larger in hollow than in hummock samples from the same sites (Price et al., 1997; Loisel et al., 2009). This higher variability can be attributed to a temporary desiccation of hollows and pools commonly occurring during summer. Due to frequently observed repeated desiccation and replenishing of pools and hollows, the range of temperature and moisture conditions are higher when a peat bog micro-environment is a hollow/pool microform. The higher variability in climatic forcing on pools and hollows is thus reflected by a larger isotopic variation in the $\delta^{13}C_{cell}$ of *Sphagnum* plants, leading to erroneous interpretation of past environmental and climatic conditions, when hollow and pool species are used for stable isotope investigations. Therefore in isotope-geochemically oriented studies, peat deposits are exclusively sampled in the relatively dry central areas of raised bogs or even on dry hummocks where ombrotrophic species like *Sphagnum magellanicum*, *Sphagnum fuscum* and *S. capillifolium* (both from section Acutifolia) are dominant (e.g. Loader et al., 2007; Lamentowicz et al., 2008, 2009; Moschen et al., 2009; Kaislahti Tillman et al., 2010). Exclusion of the $\delta^{13}C_{cell}$ values of these samples from the record, assumed to consist mainly of *Sphagnum* section *Cuspidata*, results in significant attenuation of the overall high $\delta^{13}C_{cell}$ variability (decrease of $\sim 2‰$, acrotelm samples excluded).

To summarise, the large shifts in $\delta^{13}C_{cell}$ and the $\delta^{13}C_{stem}$ time series both indicate significant environmental changes from a hummock-like microform to a much wetter hollow or even shallow pool micro-topography during the 8th and 9th century. It is also supported by a significant positive correlation (Table 5) between the $\delta^{13}C_{cell}$ time series and the macrofossil DCA axis 1 scores ($r = 0.32$, p (two-tailed) <0.01). This correlation increases further when the DCA axis 1 scores and $\delta^{13}C_{stem}$ were compared ($r = 0.528$, p (two-tailed) <0.001). It therefore appears that, bearing in mind the limitations developed above, ^{13}C-enriched values (*i.e.* relatively positive values) are in general associated with periods of increased mire surface wetness, as recorded by the positive DCA axis 1 scores, which supports the results of Loisel et al. (2010). The $\delta^{18}O_{cell}$ time series provide additional evidence for 'shallow pool phases' during the 8th to 9th and during the 13th century. However, due to the coring position at the boundary between a pronounced hummock and a hollow (in order to register the maximum amount of vegetation change), the stable isotope time series are of limited use to explain smaller changes in mire surface wetness.

Table 5
Summary of non-parametric tests for *Sphagnum* spp. composition and weighted mean $\delta^{13}C$ (‰ V-PDB) and partial correlations between standardised DCA axis 1 scores vs. mean $\delta^{13}C_{cell}$ and mean $\delta^{13}C_{stem}$. Values in bold indicate significant p values, ≤ 0.05.

	Test statistics	p
Sphagnum species/section		
Sphagnum imbricatum, *S. papillosum* & *S. s. Cuspidata*	H 7.547	**0.023**
Sphagnum imbricatum & *S. papillosum*	U 123	0.103
Sphagnum imbricatum & *S. s. Cuspidata*	U 66.5	**0.021**
S. papillosum & *S. s. Cuspidata*	U 14	0.064
DCA axis 1 vs. mean $\delta^{13}C$		
DCA axis 1 vs. mean $\delta^{13}C_{cell}$	r 0.32	**0.01**
DCA axis 1 vs. mean $\delta^{13}C_{stem}$	r 0.528	**<0.001**

4.3. Human vs. climatic signals during the last millennium

As Ti is mainly derived from natural soil dust erosion processes (e.g. Hölzer and Hölzer, 1998), it is possible to use it to calculate an atmospheric soil dust content (Shotyk et al., 1998). Because Ti is conservative, it can be assumed that its concentration in 'soil dust' is generally similar to its concentration in the upper continental crust (0.40%, McLennan, 2001) and the soils from which it is eroded. Taking into account the peat bulk density and the mean accumulation rate for a given sample, it is possible to calculate an atmospheric soil dust flux as follows:

$$\mathrm{ASD}\left(\mu g\ cm^{-2}\ y^{-1}\right) = 100/0.4 \times \mathrm{Ti}\left(\mu g\ g^{-1}\right) \times \mathrm{density}\left(g\ cm^{-3}\right) \times \mathrm{acc.\ rate}\left(cm\ y^{-1}\right)$$

Because the age/depth model and the peat accumulation rate was created using BACON, it was used to calculate the ASD flux in order to integrate the age probability distribution in the flux calculation and represent it as a grey-scales. The same approach was used to calculate the Cereal pollen fluxes by multiplying the Cereal concentration of a given sample by the density and the accumulation rate of this sample. Here, these two fluxes are used to reconstruct human activities in the area, in addition to the identification of possible climatic events.

The general Cereal increase during the Middle Ages and the first part of the industrial revolution is due to agriculture and land clearance occurring in this region of Belgium (Fig. 6b). Historical documents mention the development of villages such as Monschau (5 km east) in 1198 AD and regional but small-scale deforestation at the end of the 12th century (Letocart, 1989). These small-scale human interventions involved cutting of *Fagus* spp., which benefited *Quercus* spp. development and created small forest openings. The first occupation trace nearby the Misten bog dates back to the middle of the 13th century, when a field parcel 1 km away from the Misten bog was given to the Abbey of Reichestein (Nekrassoff, 2007) and was subsequently cultivated. Another farm was also established 5 km to the north of the Misten bog in the middle of the 14th century (Nekrassoff, 2007). These first nearby agricultural activities are well recorded in the Cereal flux, which increases from *ca.* 1220 AD to peak around 1320 AD. From the 15th century onwards, historical documents report the increase of agriculture, cattle grazing, wood cutting and charcoal making (Letocart, 1989). This gradual increase in land clearance is also recorded in the relative proportion of non-arboreal pollen, which increases from 20% around *ca.* 500 AD to 60% around *ca.* 1900 AD (Fig. 3). The Cereal flux also increases from *ca.* 1500 AD with 2 peaks at *ca.* 1540 AD and 1650 AD respectively. Then, the Cereal flux increased continuously. The upper samples are composed of living *Sphagnum* mosses, which tend to dilute the pollen content, reduce the density and therefore reduce the Cereal flux.

At a first visual correlation, the ASD flux seems similar to the Cereal flux (Fig. 6b). It therefore also reflects the increase of land clearance and agriculture in the region. These activities promote soil erosion and dust availability. However, subtle discrepancies occur between the Cereal and the ASD flux profiles. For example, the ASD profile display a distinctive peak between *ca.* 1220 AD and 1380 AD, then a second one between 1380 AD and 1620 AD. Moreover, this second peak is not associated with a change in the NAP pollen diagram. It has already been demonstrated that

climatic instabilities such as the LIA, 8.2ka event or Younger Dryas, can cause abrupt increases in ASD inputs, linked to increased wind storminess (Shotyk et al., 1998; de Jong et al., 2007, 2010; De Vleeschouwer et al., 2009; Le Roux et al., in press). However, the quantification and interpretation of such abrupt mineral increases during the last millennium require special attention, because the consequences (*i.e.* increased dust fluxes) of abrupt climatic changes are superimposed upon human impacts such as land clearance, soil use and subsequent increased erosion. Therefore, in the ASD flux profile, human impact due to land clearance and agriculture cannot be quantitatively isolated from the global signal, because an intensification of wind strength will result in an increase of transport (and deposition) of both mineral and pollen grains. There may therefore be periods of enhanced natural dust deposition superimposed upon the trend towards intensification of land use. However, it may be too speculative to go into a detailed comparison of these peaks with climatic changes, especially because they are superimposed upon a European (*ca.* 1000 AD) and local (*ca.* 1200 AD) land use trend. Therefore, these peaks occur between well-known climatic events such as the Wolf and the Spörer minima (Fig. 6b). In the future a statistical method to test synchronicities of fluxes in BACON will be developed. This should give better insight on the climatic vs. human component of the ASD flux profile.

From the 18th century onwards, systematic cuttings have affected the bog hydrology (Hindryckx, 2000). The palynological zone reconstruction based on several tree-pollen records from the edge towards the centre of the bog shows that peat accumulation may have been affected as early as the middle of the 17th century (Streel et al., 2010). DCA scores and macrofossils may therefore not reflect the natural changes in bog surface wetness during the last 300 years. The mean accumulation rate may also be affected and is indeed low (0.3 mm/y) between *ca.* 1600 AD and *ca.* 1850 AD. Therefore, interpretations are avoided for this interval, because of both the possible human induced hydrological changes of the bog and the low number of ^{14}C dates for this section of the profile, which prevents the creation of an accurate and precise age-depth chronology for this period compared to the rest of the core. From the end of the 19th century, the ASD flux increases drastically, principally because of a significant increase in mineral particles coming from various pollution sources (e.g. land clearance, intensive agriculture and mining activities). In post-1900 AD samples, the industrial revolution and its increased regional land use, but also dust-generating activities (e.g. mining), cause a dramatic increase in the ASD flux. These values are however diluted in the youngest samples, because these samples are made of living, uncompressed *Sphagnum* in the acrotelm, with high potential growth rates.

5. Summary and conclusion

The 1-m ombrotrophic peat core retrieved from the Misten bog and studied using a multiproxy approach gives insights into palaeoenvironmental changes during the last 1500 years. These are recorded as wet/dry changing conditions by macrofossils and stable C–O isotopes. In addition, a new approach of generating age-models as well as accumulation rates was adopted by using BACON software, in order to generate proxy vs. depth graphs allowing the representation of the age probability distribution. Large shifts in $\delta^{13}C_{cell}$ and the $\delta^{13}C_{stem}$ time series, occurring during the 8th and 9th century, as well as positive correlation between the $\delta^{13}C_{cell}$, $\delta^{13}C_{stem}$ and macrofossil DCA axis 1 scores, indicate changes from a hummock-like hollow/shallow pool micro-topography. The $\delta^{18}O_{cell}$ time series provide additional evidence for 'shallow pool phases' during the 8th to 9th and during the 13th century. Pollen data as well as ASD complement these findings and record human disturbance during the last millennium. The link between dust, precipitation, temperature, and humidity remains complex during periods of climatic change. More specifically, the ASD peaks do not perfectly match with the main environmental changes recorded by the macrofossil and stable isotopic results from *ca.* 1100 to 1800 AD, in addition to the human indicators such as Cereal pollen. This may be linked with the fact that the various proxies used here, have different origins, and may therefore have different response times to abrupt climatic changes. Given this, interpreting paleoenvironmental signals using both geochemical and biological proxies during the last millennium requires caution because 1) human influences are superimposed upon climatic variation, 2) events shorter than 50 years may not be detectable, even in a very well chronologically-constrained peat core.

Acknowledgements

W. Shotyk (University of Heidelberg) is warmly thanked for loaning his Wardenaar corer and for having let us use the peat-cutting facilities at the IES (University of Heidelberg, Germany). Michel Mathijs and Mona Court-Picon were of great help on the field. We thank Konrad Tudyka and Agnieszka Wiszniowska for their help with the ^{14}C sample preparation. Pascal Mertes (DNF-Belgian Forest and Nature Ministry) is also acknowledged for providing us with the official authorization for coring the Misten bog. This research was funded through the ATIS ('Absolute Time Scales and Isotope Studies for Investigating Events in Earth and Human History') Marie Curie Transfer of Knowledge project MTKD-CT-2005-029642. The WD-XRF data aquisition was made possible by Richard Bindler (Umeå University) through a research grant from the Kempe Foundation, which also provided a post doc fellowship to F. De Vleeschouwer in 2010. We thank guest editor Paul D.M. Hughes, Jonathan Nichols, and one anonymous reviewer for their useful comments on an earlier version of this manuscript.

References

Amesbury, M.J., Barber, K.E., Hughes, P., 2010. The methodological basis for fine-resolution, multiproxy reconstructions of ombrotrophic peat bog surface wetness. Boreas 10, 1–14.

Appleby, P.G., 2001. Chronostratigraphic techniques in recent sediments. In: Last, W.M., Smol, J.P. (Eds.), Tracking Environmental Change Using Lake Sediments. Basin Analysis, Coring and Chronological Techniques, vol. 1. Springer, pp. 171–203.

Barber, K.E., Langdon, P.G., 2007. What drives the peat-based palaeoclimate record? A critical test using multi-proxy climate records from northern Britain. Quaternary Science Reviews 26, 3318–3327.

Barber, K.E., 2007. Peatland records of Holocene climate change. In: Elias, S.A. (Ed.), Encyclopedia of Quaternary Science. Elsevier, Oxford, pp. 1883–1894.

Blaauw, M., Christen, J.A., 2005. Radiocarbon peat chronologies and environmental change. Applied Statistics 54, 805–816.

Blaauw, M., van der Plicht, J., van Geel, B., 2004. Radiocarbon dating of bulk peat samples from raised bogs: non-existence of a previously reported reservoir effect? Quaternary Science Reviews 23, 1537–1542.

Blaauw, M., Christen, J.A., Mauquoy, D., van der Plicht, J., Bennett, K.D., 2007. Testing the timing of radiocarbon-dated events between proxy archives. The Holocene 17, 283–288.

Blaauw, M., Bennet, K.D., Christen, J.A., 2010a. Random walk simulations of fossil proxy data. The Holocene 20, 645–649.

Blaauw, M., Wohlfarth, B., Christen, J.A., Ampel, L., Veres, D., Hughen, K., Preusser, F., Svensson, A., 2010b. Were last glacial climate events simultaneous between Greenland and France? A quantitative comparison using non-tuned chronologies. Journal of Quaternary Science 25, 387–394.

Blaauw, M., Christen, J.A., 2011. Flexible paleoclimate age-depth models using an autoregressive gamma process. Bayesian Analysis 6, 457–474.

Charman, D.J., Barber, K.E., Blaauw, M., Langdon, P.G., Mauquoy, D., Daley, T.J., Hughes, P.D.M., Karofeld, E., 2009. Climate drivers for peatland palaeoclimate records. Quaternary Science Reviews 28, 1811–1819.

Daley, T.J., Barber, K.E., Street-Perrott, F.A., Loader, N.J., Marshall, J.D., Crowley, S.F., Fisher, E.H., 2010. Holocene climate variability revealed by oxygen isotope analysis of *Sphagnum* cellulose from Walton Moss, northern England. Quaternary Science Reviews 29, 1590–1601.

Damblon, F., 1994. Les dépôts tourbeux et l'histoire de la végétation sur le plateau des Hautes Fagnes (Belgique). Annales de la Société Géologique de Belgique 117, 259–276 (In French).

de Jong, R., Schoning, K., Björck, S., 2007. Increased aeolian activity during humidity shifts as recorded in a raised bog in south-west Sweden during the past 1700 years. Climate of the Past 3, 411–422.

de Jong, R., Blaauw, M., Chambers, F.M., Christensen, T.R., De Vleeschouwer, F., Finsinger, W., Fronzek, S., Johansson, M., Kokfelt, U., Lamentowicz, M., LeRoux, G., Mitchell, E.A.D., Mauquoy, D., Nichols, J.E., Samaritani, E., van Geel, B., 2010. Peatlands and Climate. In: Dodson, J. (Ed.), Changing Climates, Earth Systems, and Society. Springer, Heidelberg, pp. 85–121.

De Vleeschouwer, F., Gérard, L., Goormaghtigh, C., Mattielli, N., Le Roux, G., Fagel, N., 2007. Last two millennia atmospheric lead and heavy metals inputs in a Belgian peat bog: regional to global human impacts. The Science of the Total Environment 377, 297–310.

De Vleeschouwer, F., Cheburkin, A., Le Roux, G., Piotrowska, N., Sikorski, J., Lamentowicz, M., Fagel, N., Mauquoy, M., 2009. Multiproxy evidence of Little Ice Age palaeoenvironmental changes in a peat bog from northern Poland. The Holocene 19, 625–637.

De Vleeschouwer, F., Sikorski, J., Fagel, N., 2010. Development of lead 210 measurement in peat using polonium extraction. A procedural comparison. Geochronometria 36, 1–8.

DeNiro, M.J., Epstein, S., 1979. Relationship between the oxygen isotope ratios of terrestrial plant cellulose, carbon dioxide, and water. Science 204, 51–53.

DeNiro, M.J., Epstein, S., 1981. Isotopic composition of cellulose from aquatic organisms. Geochimica et Cosmochimica Acta 45, 1885–1894.

Firbas, F., 1949. Späit- und nacheiszeitliche Waldgeschichte Mitteleuropas nörrdlich der Alpen. Fischer, Jena, 480 pp.

Goslar, T., Czernik, J., 2000. Sample preparation in the Gliwice Radiocarbon Laboratory for AMS ^{14}C dating of sediments. Geochronometria 18, 1–8.

Goslar, T., Czernik, J., Goslar, E., 2004. Energy ^{14}C AMS in Poznan Radiocarbon Laboratory, Poland. Nuclear Instruments and Methods in Physics Research B 223 (224), 5–11.

Hindryckx, M.-N., Streel, M., 2000. L'altération des bords de la tourbière active du Misten par l'exploitation de la tourbe pourrait dater du début du 14^{e} siècle. Hautes Fagnes 4, 95–101 (In French).

Hindryckx, M.-N., 2000. Evolution régressive de la végétation des tourbières à sphaignes en haute Ardenne. Thèse de doctorat (Sc. biologiques), Ulg. In French.

Hölzer, A., Hölzer, A., 1998. Silicon and titanium in peat profiles as indicators of human impacts. The Holocene 8, 685–696.

Kaislahti Tillman, P., Holzkämper, S., Kuhry, P., Sannel, A.B.K., Loader, N.J., Robertson, I., 2010. Stable carbon and oxygen isotopes in *Sphagnum fuscum* peat from subarctic Canada: implications for palaeoclimate studies. Chemical Geology 270, 216–226.

Kilian, M.R., van der Plicht, J., Van Geel, B., 1995. Dating raised bogs: new aspects of AMS ^{14}C wiggle matching, a reservoir effect and climatic change. Quaternary Science Reviews 14, 959–966.

Lamentowicz, M., Cedro, A., Gałka, M., Goslar, T., Miotk-Szpiganowicz, G., Mitchell, E.A.D., Pawlyta, J., 2008. Last millennium palaeoenvironmental changes from a Baltic bog (Poland) inferred from stable isotopes, pollen, plant macrofossils and testate amoebae. Palaeogeography, Palaeoclimatology, Palaeoecology 265, 93–106.

Lamentowicz, M., Milecka, K., Gałka, M., Cedro, A., Pawlyta, J., Piotrowska, N., Lamentowicz, Ł., van der Knaap, W.O., 2009. Climate- and human-induced hydrological change since AD 800 in an ombrotrophic mire in Pomerania (N Poland) tracked by testate amoebae, macrofossils, pollen, and tree-rings of pine. Boreas 38, 214–229.

Le Roux, G., De Vleeschouwer, F., 2010. Preparation of peat samples for inorganic geochemistry used as paleoenvironmental proxies. Mires and Peat 7, 1–9. Article 04.

Le Roux, G., Fagel, N., Krachler, M., Debaille, V., Stille, P., De Vleeschouwer, F., Mattielli, N., Van Der Knaap, P., Van Leeuwen, J., Shotyk, W. Dust input e climate interactions through the Holocene in Central Europe. Geology, in press.

Letocart, F., 1989. Les domaines forestiers dans le duché de Limbourg: limites, évolution et gestion des origines au XVe siècle. Msc thesis, Department of History, University of Liège, Belgium, 189 pp. (In French).

Leuenberger, M., 2007. To what extent can ice core data contribute to the understanding of plant ecological developments of the past? Terrestrial Ecology 1, 211–233.

Liégeois-Lemaitre, M., 1957. Histoire d'une forêt de Haut Plateau ardennais en vue d'une étude phytogéographique. Bulletin de la Société Royale des Sciences – Liège 26, 354–368 (In French).

Loader, N.J., McCarroll, D., van der Knaap, W.O., Robertson, I., Gagen, M., 2007. Characterizing carbon isotopic variability in *Sphagnum*. The Holocene 17, 403–410.

Loisel, J., Garneau, M., Hélie, J.-F., 2009. Modern *Sphagnum* δ^{13}C signatures follow a surface moisture gradient in two boreal peat bogs, James Bay lowlands, Québec. Journal of Quaternary Science 24, 209–214.

Loisel, J., Garneau, M., Hélie, J.-F., 2010. *Sphagnum* δ^{13}C values as indicators of palaeohydrological changes in a peat bog. The Holocene 20, 285–291.

Martin, L.H., Lang, K.C., 1933. The thermal conductivity of water. Proceedings of the Physical Society 45, 523–529.

Mauquoy, D., van Geel, B., 2007. Mire and peat macros. In: Elias, S.A. (Ed.), 2007. Encyclopedia of Quaternary Science, vol. 3. Elsevier, pp. 2315–2336.

Mauquoy, D., van Geel, B., Blaauw, M., van der Plicht, J., 2002. Evidence from northwest European bogs shows 'Little Ice Age' climatic changes driven by variation in solar activity. The Holocene 12, 1–6.

Mauquoy, D., van Geel, B., Blaauw, M., Speranza, A., van der Plicht, J., 2004. Changes in solar activity and Holocene climatic shifts derived from ^{14}C wiggle-match dated peat deposits. The Holocene 14, 45–52.

Mauquoy, D., Yeloff, D., van Geel, B., Charman, D., Blundell, A., 2008. Two decadally resolved records from north-west European peat bogs show rapid climate changes associated with solar variability during the mid-late Holocene. Journal of Quaternary Science 23, 745–763.

McLennan, S.M., 2001. Relationships between the trace element composition of sedimentary rocks and upper continental crust. Geochemistry, Geophysics, Geosystems 2, 1021. doi:10.1029/2000GC000109.

Ménot, G., Burns, S.J., 2001. Carbon isotopes in plants as climatic indicators: calibration from an altitudinal transect of ombrogenic peat bogs in Switzerland. Organic Geochemistry 31, 233–245.

Ménot-Combes, G., Burns, S.J., Leuenberger, M., 2002. Variations of ^{18}O/^{16}O in plants from temperate peat bogs (Switzerland): implications for paleoclimatic studies. Earth and Planetary Science Letters 202, 419–434.

Mormal, P., Tricot, C., 2004. Aperçu climatique des Hautes Fagnes. Institut Royal météorologique de Belgique, Publication scientifique et technique Nr36 (In French).

Moschen, R., Kühl, N., Rehberger, I., Lücke, A., 2009. Stable carbon and oxygen isotopes in sub-fossil *Sphagnum*: assessment of their applicability for palaeoclimatology. Chemical Geology 259, 262–272.

Nekrassoff, S., 2007. Images et visages des Hautes Fagnes. Evolution d'un paysage et de sa perception. Liège, Belgium, 120 pp. (In French).

O'Donnell, J.A., Romanovsky, V.E., Harden, J.W., McGuire, A.D., 2009. The effect of moisture content on the thermal conductivity of moss and organic soil Horizons from Black Spruce ecosystems in Interior Alaska. Soil Science 174, 646–651.

Pahaut, P., Oldenhove de Guertechin, F.-B., 1962. Carte des sols de la Belgique. Texte explicatif de la planchette d'Eupen 136E. Centre de cartographie des sols (IRSIA, Gent), 139 pp. (In French).

Persh, F., 1950. Zur postglazialen Wald-und Moorentwicklung im Hohen Venn. Decheniana 104, 81–93 (In German).

Price, G.D., McKenzie, J.E., Pilcher, J.R., Hoper, S.T., 1997. Carbon-isotope variation in *Sphagnum* from hummock-hollow complexes: implications for Holocene climate reconstruction. The Holocene 7, 229–233.

Reimer, P.J., Baillie, M.G.L., Bard, E., Bayliss, A., Beck, J.W., Blackwell, P.G., Bronk Ramsey, C., Buck, C.E., Burr, G., Edwards, R.L., Friedrich, M., Grootes, P.M., Guilderson, T.P., Hajdas, I., Heaton, T.J., Hogg, A.G., Hughen, K.A., Kaiser, K.F., Kromer, B., McCormac, F.G., Manning, S., Reimer, R.W., Richards, D.A., Southon, J.R., Talamo, S., Turney, C.S.M., van der Plicht, J., Weyhenmeyer, C.E., 2009. IntCal09 and Marine09 radiocarbon age calibration curves, 0–50,000 years cal BP. Radiocarbon 51, 1111–1150.

Rice, S.K., 2000. Variation in carbon isotope discrimination within and among *Sphagnum* species in a temperate wetland. Oecologia 123, 1–8.

Rinne, K.T., Boettger, T., Loader, N.J., Robertson, I., Switsur, V.R., Waterhouse, J.S., 2005. On the purification of a-cellulose from resinous wood for stable isotope (H, C and O) analysis. Chemical Geology 222, 75–82.

Shotyk, W., Weiss, D., Appleby, P.G., Cheburkin, A.K., Frei, R., Gloor, M., Kramers, J.D., Reese, S., van der Knaap, W.O., 1998. History of atmospheric lead deposition since 12,370 ^{14}C yr BP from a peat bog, Jura mountains, Switzerland. Science 281, 1635–1640.

Sikorski, J., Bluszcz, A., 2008. Application of α and γ spectrometry in the ^{210}Pb method to model sedimentation in artificial retention reservoir. Geochronometria 31, 65–75.

Sternberg, L., da, S.L., DeNiro, M.J., Savidge, R.A., 1986. Oxygen isotope exchange between metabolites and water during biochemical reactions leading to cellulose synthesis. Plant Physiology 82, 423–427.

Streel, M., De Vleeschouwer, F., Fagel, N., Gerrienne, P., Javaux, E., Luthers, C., Damblon, F., Court-Picon, M., Le Roux, G., Mauquoy, D., Piotrowska, N., Sikorski, J., Allan, M., Mattielli, N., Brack, J., Wastiaux, C., Hindrycks, M.-N., Leclercq, L., 2010. Spatio-temporal natural and anthropogenic environmental variability during the last 1500 yrs in an ombrotrophic bog (East Belgium). In: BELQUA Annual Scientific Workshop, Brussels, 2nd March 2010.

Wastiaux C., Schumacker R., 2003. Topographie de surface et de subsurfacedes zones tourbeuses des réserves naturelles domaniales des Hautes-Fagnes. Convention C60 entre le Ministère de la Région Wallonne, Direction générale des Ressources naturelles et de l'Environnement, et l'Université de Liège. 52 p. +annexes (In French).

Wardenaar, E.P.C., 1986. A new hand tool for cutting peat profiles. Canadian Journal of Botany 65, 1772–1773.

Williams, T.G., Flanagan, L.B., 1996. Effect of changes in water content on photosynthesis, transpiration and discrimination against $^{13}CO_2$ and C^{18}O^{16}O in *Pleurozium* and *Sphagnum*. Oecologia 108, 38–46.

Wissel, H., Mayr, C., Lücke, A., 2008. A new approach for the isolation of cellulose from aquatic plant tissue and freshwater sediments for stable isotope analysis. Organic Geochemistry 39, 1545–1561.

Yeloff, D., Mauquoy, D., 2006. The influence of vegetation composition on peat humification: implications for palaeoclimatic studies. Boreas 35, 662–673.

Zanazzi, A., Mora, G., 2005. Paleoclimate implications of the relationship between oxygen isotope ratios of moss cellulose and source water in wetlands of Lake Superior. Chemical Geology 222, 281–291.

Zonderyan, A., Poletti, M., Purcell, C.R., Sparks, R.J., 2007. Accelerator and beamline upgrades at the AMS facility of GNS Science, New Zealand. Nuclear Instruments and Methods in Physics Research B 259, 47–49.